Simulating Electron Transfer Attachment to a Positively Charged Model Peptide†

Iwona Anusiewicz,‡ Joanna Berdys-Kochanska,§ Piotr Skurski,‡,§ and Jack Simons*,‡

Department of Chemistry and Henry Eyring Center for Theoretical Chemistry, University of Utah, Salt Lake City, Utah 84112, and Department of Chemistry, University of Gdansk, Sobieskiego 18, 80-952, Gdansk, Poland

Received: June 1, 2005; In Final Form: August 10, 2005

Ab initio electronic structure methods, including stabilization method tools for handling electronically metastable states, are used to treat a model system designed to probe the electron-transfer event characterizing electron-transfer dissociation (ETD) mass spectroscopic studies of peptides. The model system consists of a cation $H_3C-(C{=}O)NH-CH_2-CH_2-NH_3^+$, containing a protonated amine site and an amide site, that undergoes collisions with a CH_3^- anion. Cross-sections for electron transfer from CH_3^- to the protonated amine site are shown to exceed those for transfer to the Coulomb-stabilized amide site by 2 orders of magnitude. Moreover, it is shown that the fates of the amine-attached and amide-attached species are similar in that both eventually lead to the same carbon-centered radical species $H_3C-(^{\bullet}C-OH)NH-CH_2-CH_2-NH_2$, although the reaction pathways by which the two species produce this radical are somewhat different. The implications for understanding peptide fragmentation patterns under ETD conditions are also discussed in light of this work's findings.

I. Introduction

In electron capture dissociation[1] (ECD) or electron-transfer dissociation[2] (ETD) mass spectroscopy experiments, low energy electrons are believed to first attach (primarily) to positively charged sites within the gas-phase sample. These sites include, for example, protonated amine or guanidinium groups on side chains as well as protonated amide units along the backbone. When a side-chain positive group is proximal to (e.g., as when involved in hydrogen bonding) either the oxygen atom of an amide unit or a disulfide bond, the nascent hypervalent radical formed when an electron attaches can subsequently transfer an H atom to either the carbonyl oxygen or a sulfur atom to produce the radical species shown in Schemes 1 and 2 where the side chain is assumed to contain a protonated amine.

Once the O−H or S−H bond is formed, subsequent cleavage of either the N−C_α or S−S bond can occur to produce the ECD-characteristic fragmentation products shown as the final species in Schemes 1 and 2. The very selective cleavage of these two kinds of bonds observed in ECD and ETD spectra are very positive attributes of these two probes of primary sequence. One of the N−C_α bond cleavage's driving forces is the formation of the C═N π bond to form the closed-shell species labeled c in Scheme 2, after which rearrangement to form the $-C{=}O(-NH_2)$ species can occur.

In an earlier study,[3] we investigated an alternative pathway by which S−S bonds could be cleaved in peptides. In particular, following our studies[4−7] of how proximal positive charges can render exothermic direct electron attachment to antibonding orbitals, we considered the possibility that electron transfer (or attachment) could take place directly into an S−S σ^* orbital. Of course, it is known[8] that direct attachment to this orbital in the absence of any stabilizing Coulomb effects is endothermic by ca. 1.0 eV. However, we showed that the presence of any nearby positively charge group (e.g., a $-NH_3^+$ unit or a sodiated analogue $-NH_2Na^+$) can differentially stabilize the S−S σ^* electron-attached state by an amount 14.4 eV/R that can be estimated by knowing the distance R (Å) from the S−S bond to the positive site.

SCHEME 1

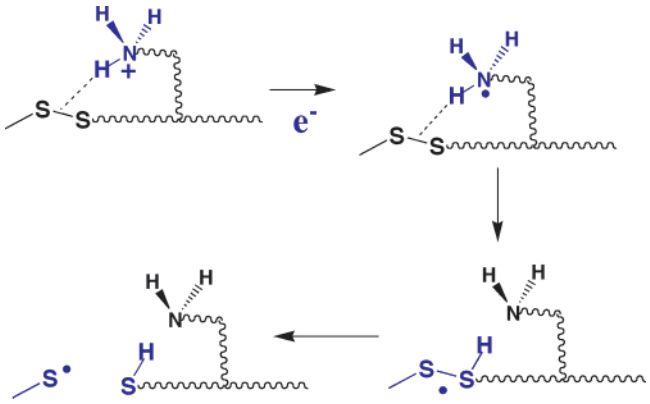

In the study of ref 3, we used H_3C^- as a model electron-transfer agent because

(i) it is a small enough anion to allow us to carry out good quality ab initio calculations,

(ii) its center of negative charge is localized enough for us to confidently measure the distance X between it and the $-NH_3^+$ site, and

(iii) it has a small electron binding energy (ca. 0.1 eV) so results obtained on it may also apply to the ECD case (i.e., ECD may be thought of as equivalent to electron transfer from an anion of zero binding energy).

As our model disulfide-containing compound, we chose Me−SS−$CH_2-CH_2-NH_3^+$, which, in its most extended structure,

† Part of the special issue "William Hase Festschrift".

* Corresponding author. E-mail: simons@chem.utah.edu.
‡ University of Utah.
§ University of Gdansk.

10.1021/jp052914j CCC: $33.50
Published on Web 09/20/2005

SCHEME 2

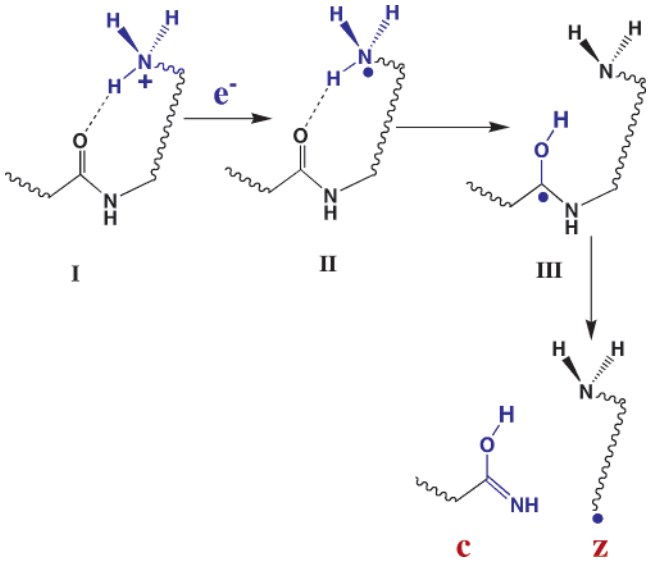

has the nitrogen atom ca. 4.8 Å from the midpoint of the S−S bond. Such a positive charge generates >3 eV of stabilizing Coulomb potential at the SS bond site, thus rendering direct attachment of an electron to the S−S σ^* orbital exothermic by > 2 eV.

The assumptions underlying our earlier simulations were as follows:

1. We had to treat three distinct electronic states:

(a) An "ion-pair state" involving Me−SS−CH_2−CH_2−NH_3^+ and CH_3^-, whose energy varies approximately as 14.4 eV/X, where X is the distance from the nitrogen atom to the methyl anion's carbon.

(b) A second state involving the hypervalent species Me−SS−CH_2−CH_2−NH_3 (with the electron transferred to the $-NH_3^+$ site) and neutral CH_3, whose energy is quite independent of X for large X.

(c) A third in which an electron has transferred from the methyl anion to the S−S σ^* orbital to give the neutral Me−SS^-−CH_2−CH_2−NH_3^+ and neutral CH_3; again, the energy of this state is relatively independent of X for large X.

2. A resonant electron-transfer mechanism could be used to compute the rates and cross-sections for transfer from CH_3^- to form either the hypervalent species or the S−S σ^* attached species.

3. We could use Landau−Zener theory to estimate these rates once we found the geometries (i.e., values of X) at which the potential curves of the first and second or first and third states described above cross.

These curve crossings appropriate to the S−S bond cleavage case are depicted qualitatively in Figure 1.

In ref 3 we found the curve crossing positions by carrying out ab initio calculations on the three electronic states characterized above. Pairs of energy curves at the two crossings we found are shown in Figure 2 where we also see the minimum-energy splitting between the curves.

Knowing the splitting $H_{1,2}$ as well as the difference in slopes ΔF for each curve crossing as well as the relative velocity v of the Me−SS−CH_2−CH_2−NH_3^+ + CH_3^- ion pair as they enter the crossing, we used the Landau−Zener probability expression

$$P = 1 - \exp(-2\pi H_{1,2}^2/(\hbar \Delta F v)) \qquad (1)$$

to compute the probability that such a collision would lead to electron transfer. The cross-sections for forming the σ^*- and

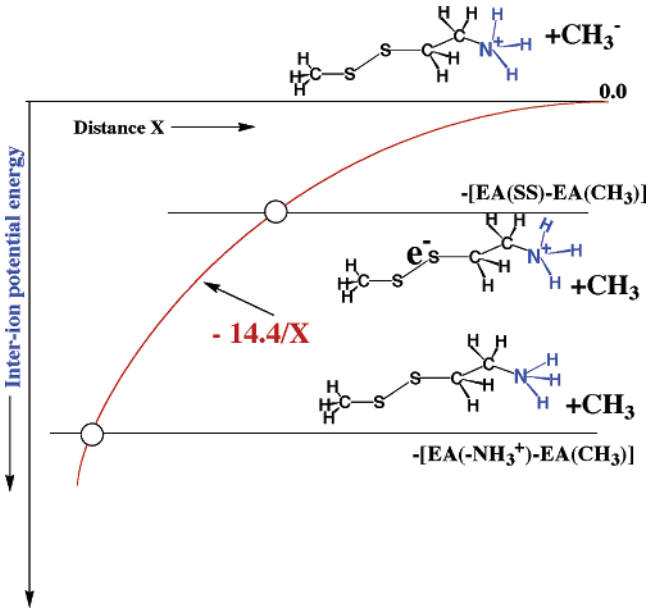

Figure 1. Energies of the ion-pair state (top at large X), the S−S σ^* attached state (middle), and hypervalent state (bottom) as functions of the distance X between the methyl anion's carbon atom and the nitrogen atom.

hypervalent-attached states were then computed as

$$\sigma = \pi X_C^2 P \qquad (2)$$

for which we obtained $\sigma \approx 10^{-14}$−10^{-16} cm^2 for the hypervalent site and $\sigma \approx 10^{-16}$−10^{-17} cm^2 for the SS σ^* site.[9] It is worth noting that although the crossing of the σ^* site occurs at larger X (which tends to enhance its cross-section via the X_C^2 factor of eq 2), the splitting matrix element $H_{1,2}$ for this site is sufficiently smaller than that for the hypervalent site to more than offset the X_C^2 factor. $H_{1,2}$ is smaller for the σ^* site because the overlap between the CH_3^- anion's valence orbital and the S−S σ^* orbital is quite small at $X = 8.2$. In contrast, the overlap of the CH_3^- and $-NH_3^+$ orbitals at $X_C = 3.6$ Å is much larger.

These data allowed us to suggest that electron transfer (from CH_3^-, and, by extrapolation, from free electrons as in ECD) to a protonated amine site is 10−100 times as likely to occur as to an S−S σ^* site that is Coulomb stabilized to the extent that attachment to it is ca. 2 eV exothermic. If the protonated amine group were more distant from the S−S bond, the S−S σ^* orbital would have a smaller EA and thus the corresponding crossing would occur at even larger X values. This likely (because the $H_{1,2}$ value would probably be even smaller than that for our model compound) would produce an even smaller cross-section for electron attachment. In contrast, if the positive site were closer to the S−S bond than the 4.8 Å in our compound, the cross-section for attachment to this bond would be larger.

II. Goals of This Work

In the present effort, we extend our earlier study of S−S bond attachment to consider the relative rates at which electron transfer occurs to a protonated amine site or to a Coulomb-stabilized amide (OCN) bond site in the model compound shown in Scheme 3. This cation is similar to that used in our study of S−S bond cleavage and has an amide unit in place of the S−S fragment of the compound discussed in the preceding section.

As in our earlier study, the primary goal of this portion of the work is to determine the relative cross-sections for producing amine-attached or amide-attached species, both of which are expected to subsequently produce N−C_α bond cleavage. The

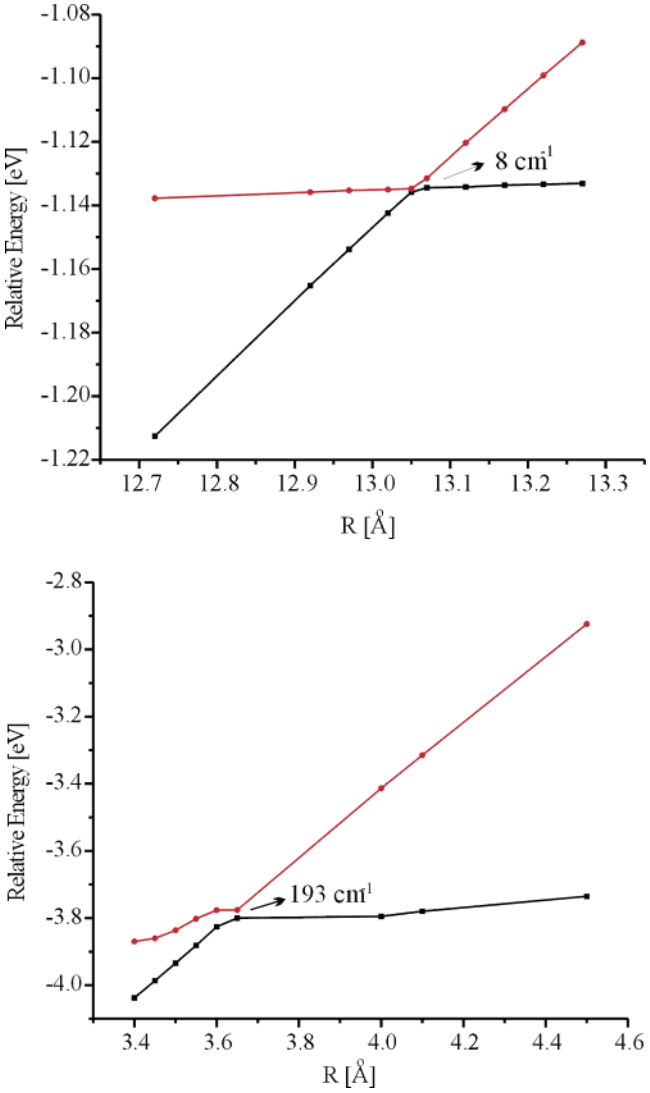

Figure 2. SCF-level energies of the ion-pair and σ^*-attached (top) states and of the ion-pair and hypervalent-attached (bottom) states obtained in ref 3. In the bottom plot, the distance R is measured from the nitrogen atom to the carbon of CH_3^-. In the top plot, R measures the distance from the carbon of CH_3^- to the midpoint of the S−S bond (which is ca. 4.8 Å from the nitrogen atom).

SCHEME 3

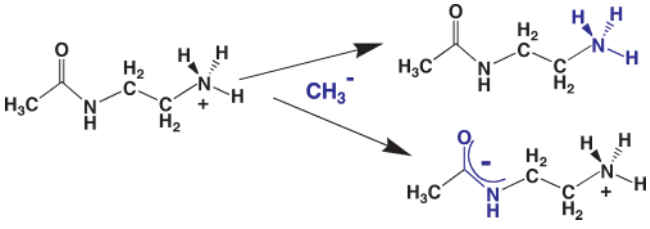

hypervalent species does so by first transferring an H atom to the carbonyl oxygen to generate a carbon-centered radical as in Scheme 2; the amide-attached species does so by transferring a proton from the $-NH_3^+$ group to the amide oxygen generating the same carbon-centered radical.

In addition, we have considered here whether it is possible (and, if so, at what rates) for an electron initially captured at the hypervalent site to transfer to the amide site (or vice versa) as the distance between the amine nitrogen and amide carbon atoms varies (e.g., due to thermal motions). Such intramolecular electron-transfer events are illustrated in Scheme 4.

SCHEME 4

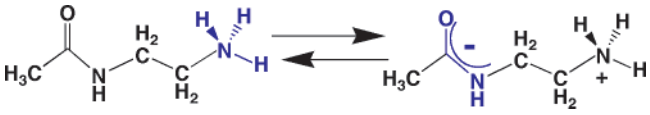

When considering such processes, one needs to search for crossings of the energies of the ion-pair state shown on the right in Scheme 4 and the hypervalent state shown on the left as a function of the amine−amide distance.

III. Methods

The geometries of the species studied in this work were optimized either at the Hartree−Fock self-consistent field (SCF) level or at the second-order Møller−Plesset (MP2) level using 6-31+G(d) basis sets.[10] In the following section where we present our results, we specify whether SCF or MP2 treatments apply. To generate the energy profiles through the potential energy surfaces of the various species examined here, we kept one geometrical variable (the distance between two atoms) frozen while relaxing the other degrees of freedom to minimize the electronic energy. Because the methods we used are based on an unrestricted Hartree−Fock (UHF) starting point, it is important to make sure that little, if any, artificial spin contamination enters into the final wave functions. We computed the expectation value $\langle S^2 \rangle$ for species studied in this work and found values not exceeding 0.77 (after annihilation) in all open-shell doublet neutral cases. For three cases (specified in section IV when discussed), we had to make use of a stabilization procedure described elsewhere[11] because the electronic states of these species are unstable with respect to electron autodetachment. The Gaussian 03 suite of programs[12] was used to perform all of the calculations, and the Molden visualization program[13] was employed to examine the molecular orbitals and to construct some of the molecular structures shown.

IV. Results

A. Electron-Transfer Cross-Sections. First, we examined the processes in which an electron is transferred from a CH_3^- anion to either the protonated amine site or the Coulomb-stabilized[14] amide site of our model cation $H_3C-(C{=}O)NH-CH_2-CH_2-NH_3^+$. In Figure 3, we show the energies of the ion-pair state $H_3C-(C{=}O)NH-CH_2-CH_2-NH_3^+\cdots CH_3^-$ (representing the initial state in the ETD collision), the amide bond-attached state $H_3C-(C-O^-)NH-CH_2-CH_2-NH_3^+\cdots CH_3$, and the amine-attached Rydberg state $H_3C-(C{=}O)NH-CH_2-CH_2-NH_3\cdots CH_3$ as functions of the distance R between the carbon atom in CH_3^- and the amine nitrogen atom. In these calculations, when the CH_3^- ion is far away, the $H_3C-(C{=}O)NH-CH_2-CH_2-NH_3^+$ cation adopts an equilibrium geometry with the protonated amine group in close proximity[14] to the oxygen atom of the amide site, as also shown in Figure 3. As the CH_3^- ion approaches, it is attracted by the strong Coulomb force toward the positive $-NH_3^+$ site, as expected. When computing the energy of the amide-attached state, we had to use the stabilization process described in ref 4 (for all values of R). We also had to use the stabilization method to compute the energies of the amine-attached state for distances $R < 3.9$ Å where this state lies above the ion-pair state.

Clearly, the energy profile of the ion-pair state follows the expected 14.4 eV/R Coulomb behavior, and the other two states have energies that are very independent of R until significant overlap of the $-NH_3$ and CH_3^- valence orbitals develops (e.g., near $R = 10$ Å). The relative velocities[15] v and slope differences ΔF needed to compute the probabilities (see eq 1) for hopping

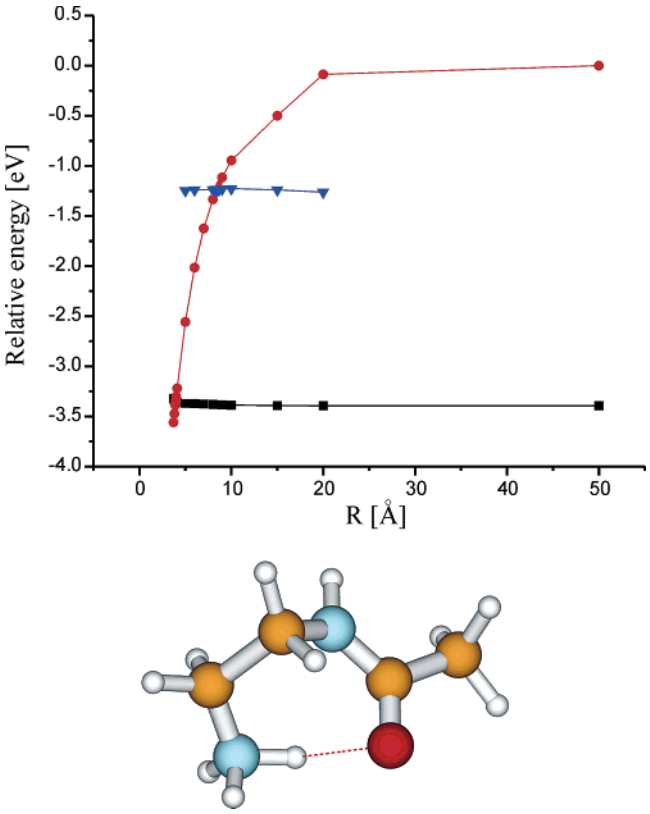

Figure 3. SCF-level energies of $H_3C-(C=O)NH-CH_2-CH_2-NH_3^+\cdots CH_3^-$ (circles), $H_3C-(C-O^-)NH-CH_2-CH_2-NH_3^+\cdots CH_3$ (triangles), and $H_3C-(C=O)NH-CH_2-CH_2-NH_3\cdots CH_3$ (squares) as functions of the CH_3^- carbon to amine nitrogen distance R. The zero of energy is taken as the energy of the $H_3C-(C=O)NH-CH_2-CH_2-NH_3^+\cdots CH_3^-$ species at $R = 50$ Å. The bottom figure shows the structure of the $H_3C-(C=O)NH-CH_2-CH_2-NH_3^+$ cation when the CH_3^- anion is far away.

from the ion-pair state to either the amide-bound or Rydberg-bound state can easily be obtained from the data represented in Figure 3.

To obtain the coupling matrix elements $H_{1,2}$ appropriate to each of the surface transitions we wish to examine, we computed the energies of the pairs of states undergoing crossings in the regions near $R = 4$ Å and $R = 8$ Å. In Figure 4, we show these curves in these regions where they actually undergo avoided crossings; it is from their distances of closest approach (splitting) that we extract the values of $H_{1,2}$ as splitting/2 $= H_{1,2}$.

We also computed the splittings at the MP2 level and, similar to what we found in our study of S−S bond cleavage, they are each ca. 50% smaller than at the SCF level.

Using the SCF-level $H_{1,2}$ and v, and ΔF data from our ab initio energy surfaces, we computed, using eqs 1 and 2, probabilities and cross-sections for the ion-pair to amide-attached and ion-pair to amine-attached Rydberg transitions and obtained:

$$P_{\text{amide}} = 5.5 \times 10^{-4} \quad (3a)$$

$$P_{\text{Rydberg}} = 4.6 \times 10^{-3} \quad (3b)$$

$$\sigma_{\text{amide}} = 3.2 \times 10^{-3}\ \text{Å}^2 \quad (3c)$$

$$\sigma_{\text{Rydberg}} = 2.7 \times 10^{-1}\ \text{Å}^2 \quad (3d)$$

Using the $H_{1,2}$ matrix elements obtained from MP2-level calculations, each of these cross-sections are predicted to be

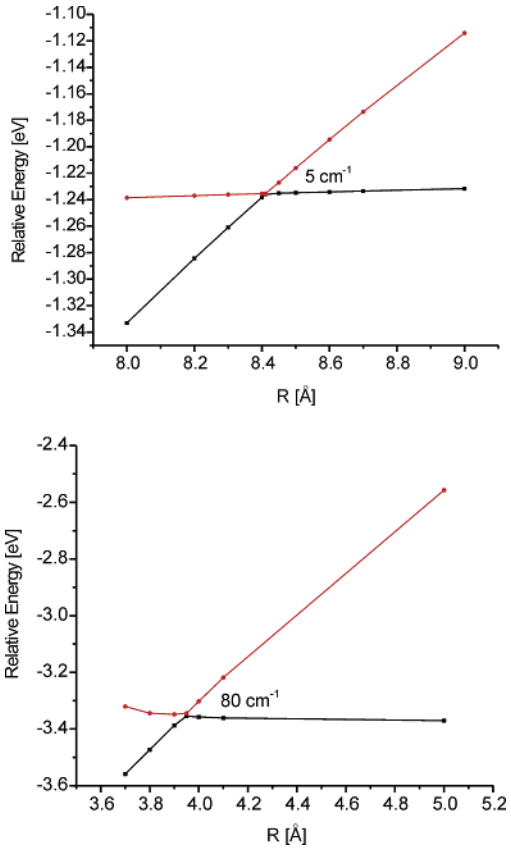

Figure 4. Plots of the SCF energies of the ion-pair and amide-attached states (top), the ion-pair and amine-attached states (below) showing the splittings (closest-approach energy).

SCHEME 5

ca. 25% of the values quoted in eq 3, but their relative sizes remain essentially unchanged.

We conclude[16] from these data that direct electron transfer to the amide site will occur at a rate approximately 100 times less than that for transfer to the protonated amine site. Therefore, it is likely that N−C_α bond cleavage, as illustrated in Scheme 2, will be initiated by electron attachment to the positive $-NH_3^+$ site. Only when this site is not in close proximity (and thus not able to transfer an H atom to the amide's oxygen atom as shown in Scheme 2), is bond cleavage more likely to begin with electron attachment at the amide site. As we discuss later, if an electron were to attach to the amide site, N−C_α bond cleavage can occur by a process shown in Scheme 5 in which a proton migrates from the protonated amine site to the negative oxygen center after or during which the N−C_α bond cleaves.

B. Fates of the Amide- and Amine-Attached Species. We also considered what is likely to happen once an electron is transferred either to the protonated amine site or to the Coulomb-stabilized amide site. In particular, we examined the energy profiles for

(a) the process shown in Scheme 4 in which the attached electron can transfer from one site to the other as the distance between the two sites undergoes dynamical fluctuations (e.g., through thermal excitation);

(b) a process in which an H atom is transferred from the nascent $-NH_3$ Rydberg species to the proximal amide oxygen atom; and

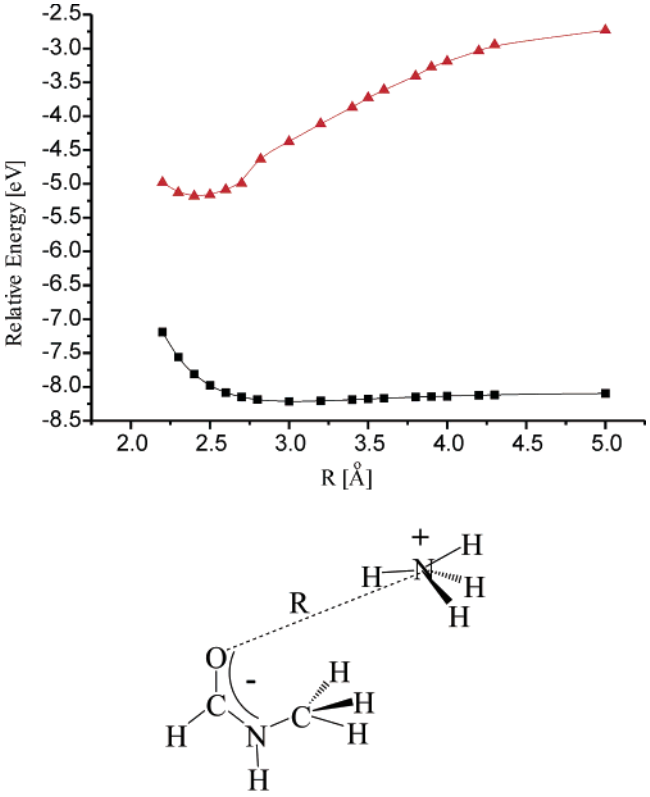

Figure 5. The top figure shows the SCF-level energies of the amide-attached (top) and amine-attached (bottom) states of the model system shown in the lower figure as functions of the N-to-O distance *R*.

SCHEME 6

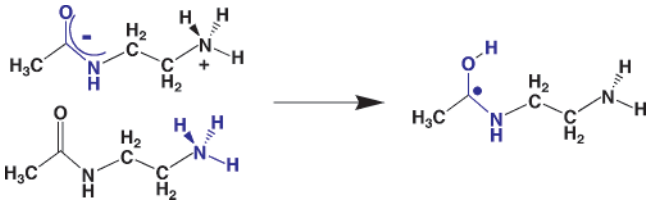

(c) a process in which a proton is transferred from the $-NH_3^+$ site to the nascent amide-attached site.

The latter two processes are illustrated in Scheme 6.

To examine the intramolecular electron transfer process illustrated in Scheme 4, we used a model system composed of the two fragments shown in Figure 5. We chose to use this system to allow the amide and amine sites to approach as closely as possible by eliminating all bond-strain effects that would arise had we used the intact fragment of Scheme 6. The energies of the amide-attached and amine-attached states of this compound as functions of the distance *R* between the amine nitrogen and the amide oxygen atoms are also shown in Figure 5. In computing the energy of the amide-attached ion-pair state, we had to employ the stabilization method as discussed in the Methods.

These data show that there is no interfragment distance at which the amide-attached and amine-attached surfaces intersect. The amide-attached state indeed decreases in energy as *R* decreases, as expected on the basis of its ion-pair character. However, it appears that repulsions between the amide and amine groups arise before the curves can cross. This suggests that once an electron transfers from CH_3^- either to the protonated amine site or to a Coulomb-stabilized amide site, it will remain on that site rather than undergo a subsequent intramolecular transfer to the other site.

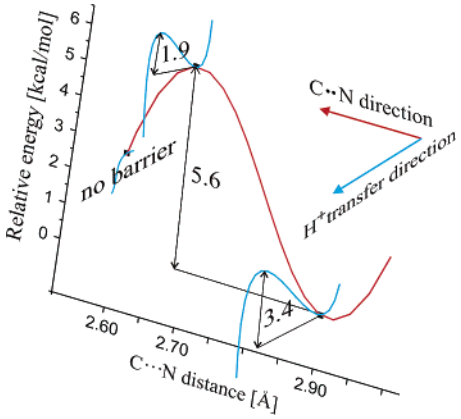

Figure 6. MP2-level energy profile for proton transfer from the protonated amine site of the amide-attached species $H_3C-(C-O^-)-NH-CH_2-CH_2-NH_3^+$ to generate the carbon-centered radical $H_3C-(^\bullet C-OH)NH-CH_2-CH_2-NH_2$.

We also examined a pathway along which the amide-attached ion-pair state of the original model compound $H_3C-(C-O^-)-NH-CH_2-CH_2-NH_3^+$ could undergo intramolecular proton transfer to generate the carbon-centered radical $H_3C-(^\bullet C-OH)-NH-CH_2-CH_2-NH_2$. We computed the energy of this state along a sequence of geometries in which we varied the amide carbon to amine nitrogen distance and (at each such distance) calculated the energy required to displace a proton from the amine site to the carbonyl oxygen (while minimizing the energy with respect to all other geometrical parameters). Figure 6 shows how the energy of this state varies as functions of these two displacements.

These data suggest that once the amide-attached species $H_3C-(C-O^-)NH-CH_2-CH_2-NH_3^+$ is formed and accesses its equilibrium geometry (at which the amine nitrogen to amide carbon distance is 2.9 Å), a barrier of only ca. 3 kcal mol^{-1} must be overcome to transfer a proton to the amide oxygen site to generate the carbon-centered radical $H_3C-(^\bullet C-OH)NH-CH_2-CH_2-NH_2$. Even if the C···N distance is compressed (e.g., by thermal motions) to near 2.7 Å (which requires ca. 6 kcal mol^{-1}) or to near 2.6 Å (where the proton spontaneously migrates to the carbonyl oxygen), at least 3 kcal mol^{-1} is needed to effect the proton transfer and generate $H_3C-(^\bullet C-OH)NH-CH_2-CH_2-NH_2$.

Finally, we also examined a pathway along which the amine-attached state of the original model compound $H_3C-(C=O)-NH-CH_2-CH_2-NH_3$ could undergo intramolecular H atom transfer to generate the same carbon-centered radical $H_3C-(^\bullet C-OH)NH-CH_2-CH_2-NH_2$. In particular, we varied the amide oxygen to amine nitrogen distance and calculated the energy required to displace an H atom from the amine site to the amide's carbonyl oxygen (while minimizing the energy with respect to all other geometrical parameters). Figure 7 shows how the energy of this state varies as functions of these two displacements.

These data suggest that once the amine-attached species $H_3C-(C=O)NH-CH_2-CH_2-NH_3$ is formed and accesses its equilibrium geometry (at which the amine nitrogen to amide oxygen distance is 3.0 Å), a barrier of ca. 11 kcal mol^{-1} must be overcome to transfer an H to the amide oxygen site to generate the carbon-centered radical $H_3C-(^\bullet C-OH)NH-CH_2-CH_2-NH_2$. If the N···O distance is compressed (e.g., by thermal motions) to near 2.4 Å (which requires ca. 8 kcal mol^{-1}), an additional 12 kcal mol^{-1} is needed to effect the H atom transfer and generate $H_3C-(^\bullet C-OH)NH-CH_2-CH_2-NH_2$. Thus, it

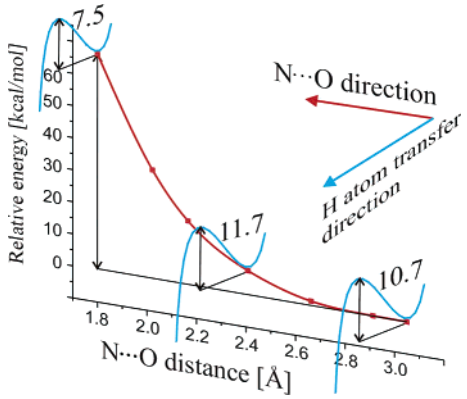

Figure 7. MP2-level energy of the amine-attached species as a function of the amine nitrogen to amide oxygen distance showing the energy profile along paths involving migrating an H atom from the amine site to the carbonyl oxygen.

appears that the amine-attached species can generate the carbon-centered radical but must pass over a barrier of ca. 11 kcal mol^{-1} to do so.

V. Summary

The primary findings of this work can be summarized as follows:

1. Electron transfer from an anion such as CH_3^- (i.e., a small ion with a small electron binding energy) to the protonated amine site of $H_3C-(C{=}O)NH-CH_2-CH_2-NH_3^+$ occurs with a cross-section $\sigma \approx 10^{-1}$ Å^2 approximately 2 orders of magnitude larger than direct electron transfer to this cation's the Coulomb-stabilized amide site for which $\sigma \approx 10^{-3}$ Å^2.

2. Once an electron is bound to either the amide site or the protonated amine site, it is not likely that thermal motions (causing the amide and amine sites to approach one another) will cause the electron to be transferred to the other site.

3. Once formed, the amine-attached Rydberg species $H_3C-(C{=}O)NH-CH_2-CH_2-NH_3$ can transfer an H atom to the carbonyl oxygen atom to form the carbon-centered radical $H_3C-(^{\bullet}C-OH)NH-CH_2-CH_2-NH_2$ but a barrier of ca. 11 kcal mol^{-1} must be surmounted.

4. Once formed, the amide-attached ion-pair species $H_3C-(C-O^-)NH-CH_2-CH_2-NH_3^+$ can transfer a proton to the carbonyl oxygen atom by surmounting a small 3 kcal mol^{-1} barrier to generate the same carbon-centered radical $H_3C-(^{\bullet}C-OH)NH-CH_2-CH_2-NH_2$.

5. As earlier workers found,[1] once this carbon-centered radical is formed by either of the processes just discussed, subsequent $N-C_\alpha$ bond cleavage requires crossing a barrier[1j] of ca. 10 kcal mol^{-1} upon which the characteristic c and z fragments of Scheme 2 can be formed.

Acknowledgment. This work was supported by NSF Grant No. 0240387 to J.S. and by the Polish State Committee for Scientific Research (KBN), Grant No. DS/8371-4-0137-5 to P.S. Significant computer time provided by the Center for High Performance Computing at the University of Utah and by the Academic Computer Center in Gdansk (TASK) is also gratefully acknowledged.

References and Notes

(1) (a) Zubarev, R. A.; Kelleher, N. L.; McLafferty, F. W. *J. Am. Chem. Soc*. **1998**, *120*, 3265−3266. (b) Zubarev, R. A.; Kruger, N. A.; Fridriksson, E. K.; Lewis, M. A.; Horn, D. M.; Carpenter, B. K.; McLafferty, F. W. *J. Am. Chem. Soc.* **1999**, *121*, 2857−2862. (c) Zubarev, R. A.; Horn, D. M.; Fridriksson, E. K.; Kelleher, N. L.; Kruger, N. A.; Lewis, M. A.; Carpenter, B. K.; McLafferty, F. W. *Anal. Chem*. **2000**, *72*, 563−573. (d) Zubarev, R. A.; Haselmann, K. F.; Budnik, B.; Kjeldsen, F.; Jensen, F. *Eur. J. Mass Spectrom.* **2002**, *8*, 337. Much of the pioneering work aimed at understanding the mechanism(s) by which ECD operates has been reported in ref 1 and by the Turecek and Uggerud groups in, for example: (e) Syrstad, E. A.; Turecek, F. *J. Phys. Chem*. **2001**, *A105*, 11144-1115; (f) Turecek, F.; Syrstad, E. A. *J. Am. Chem. Soc* **2003**,. *125*, 3353−3369; (g) Turecek, F.; Polasek, M.; Frank, A.; Sadilek, M. *J. Am. Chem. Soc*. **2000**, *122*, 2361−2370. (h) Syrstad, E. A.; Stephens, D. D.; Turecek, F. *J. Phys. Chem*. **2003**, *A107*, 115. (i) Turecek, F. *J. Am. Chem. Soc.* **2003**, *125*, 5954. (j) Syrstad, E. A. and Truecek, F. *Am. Soc. Mass. Spectrom.* **2004**, *16*, 208−224. (k) Uggerud, E. *Int. J. Mass. Spectrom*. **2004**, *234*, 45−50.

(2) (a) Syka, J. E. P.; Coon, J. J.; Schroeder, M. J.; Shabanowitz, J.; Hunt, D. F. *Proc. Natl. Acad. Sci*. **2004**, *101*, 9528−9533. (b) Coon, J. J.; Syka, J. E. P.; Schwartz, J. C.; Shabanowitz, J.; Hunt, D. F. *Int. J. Mass Spectrom*. **2004**, *236*, 33−42.

(3) Iwona Anusiewicz, Joanna Berdys-Kochanska, and Jack Simons. The Electron Attachment Step in Electron Capture (ECD) and Electron-Transfer Dissociation (ETD). *J. Phys. Chem*., in press.

(4) Sawicka, A.; Skurski, P.; Hudgins, R. R.; Simons, J. *J. Phys. Chem. B* **2003**, *107*, 13505−13511.

(5) Monika Sobczyk, Piotr Skurski, and Jack Simons. Dissociative Low-Energy Electron Attachment to the C − S Bond of H_3C-SCH_3 Influenced by Coulomb Stabilization. *Adv. Quantum Chem*., in press.

(6) Sawicka, A.; Berdys-Kochaska, J.; Skurski, P.; Simons, J. *Int. J. Quantum Chem*. **2005**, *102*, 838−846.

(7) Anusiewicz, I.; Berdys, J.; Sobczyk, M.; Sawicka, A.; Skurski, P.; Simons, J. *J. Phys. Chem. A* **2005**, *109*, 250−258.

(8) Dezarnaud-Dandine, C.; Bournel, F.; Troncy, M.; Jones, D.; Modelli, A. *J. Phys. B: At. Mol. Opt. Phys*. **1998**, *31*, L497-L502.

(9) The range of values derives from our using both the self-consistent field (SCF) and second-order Møller−Plesset methods to compute the three electronic energy curves.

(10) (a) McLean, A. D.; Chandler, G. S. *J. Chem. Phys*. **1980**, *72*, 5639−5648**.** (b) Krishnan, R.; Binkley, J. S.; Seeger, R.; Pople, J. A. *J. Chem. Phys*. **1980**, *72*, 650−654.

(11) Hazi, A. U.; Taylor, H. S. *Phys. Rev*. **1970**, *A1*, 1109. Simons, J. *J. Chem. Phys*. **1981**, *75*, 2465. Frey, R. F.; Simons, J. *J. Chem. Phys*. **1986**, *84*, 4462.

(12) Frisch, M. J.; Trucks, G. W.; Schlegel, H. B.; Scuseria, G. E.; Robb, M. A.; Cheeseman, J. R.; Montgomery, J. A., Jr.; Vreven, T.; Kudin, K. N.; Burant, J. C.; Millam, J. M.; Iyengar, S. S.; Tomasi, J.; Barone, V.; Mennucci, B.; Cossi, M.; Scalmani, G.; Rega, N.; Petersson, G. A.; Nakatsuji, H.; Hada, M.; Ehara, M.; Toyota, K.; Fukuda, R.; Hasegawa, J.; Ishida, M.; Nakajima, T.; Honda, Y.; Kitao, O.; Nakai, H.; Klene, M.; Li, X.; Knox, J. E.; Hratchian, H. P.; Cross, J. B.; Bakken, V.; Adamo, C.; Jaramillo, J.; Gomperts, R.; Stratmann, R. E.; Yazyev, O.; Austin, A. J.; Cammi, R.; Pomelli, C.; Ochterski, J. W.; Ayala, P. Y.; Morokuma, K.; Voth, G. A.; Salvador, P.; Dannenberg, J. J.; Zakrzewski, V. G.; Dapprich, S.; Daniels, A. D.; Strain, M. C.; Farkas, O.; Malick, D. K.; Rabuck, A. D.; Raghavachari, K.; Foresman, J. B.; Ortiz, J. V.; Cui, Q.; Baboul, A. G.; Clifford, S.; Cioslowski, J.; Stefanov, B. B.; Liu, G.; Liashenko, A.; Piskorz, P.; Komaromi, I.; Martin, R. L.; Fox, D. J.; Keith, T.; Al-Laham, M. A.; Peng, C. Y.; Nanayakkara, A.; Challacombe, M.; Gill, P. M. W.; Johnson, B.; Chen, W.; Wong, M. W.; Gonzalez, C.; Pople, J. A. *Gaussian 03*, revision A.1; Gaussian, Inc.: Wallingford, CT, 2004.

(13) Schaftenaar, G.; Noordik, J. H. MOLDEN: a pre- and postprocessing program for molecular and electronic structures, *J. Comput.-Aided Mol. Design* **2000**, *14*, 123.

(14) At the equilbrium geometry of $H_3C-(C{=}O)NH-CH_2-CH_2-NH_3^+$, the amine nitrogen is ca. 2.6 Å away from the carbonyl oxygen, so the Coulbomb stabilization energy is ca. 14.4/2.6 = 5.5 eV. When $H_3C-(C{=}O)NH-CH_2-CH_2-NH_3^+$ is fully extended, this distance increases to 4.9 Å, so the Coulomb stabilization is 2.9 eV.

(15) As in our earlier study of S−S bond cleavage, we assume that the peptide cation and CH_3^- anion have essentially zero relative velocity prior to being accelerated toward one another by their Coulomb attraction.

(16) Because we used an anion with a small electron binding energy and a small physical "size", we can speculate that our findings may also apply to the ECD situation (i.e., capture of a free electron should not be too much different from transfer of an electron from an anion with a small binding energy).